LINEAR ELASTIC FRACTURE MECHANICS INTERPRETATION OF CRACK GROWTH BEHAVIOUR IN FRETTING FATIGUE

U.S. FERNANDO, M.W. BROWN and K.J. MILLER
SIRIUS, Faculty of Engineering, University of Sheffield, Mappin Street, Sheffield S1 3JD, UK

ABSTRACT

Fretting fatigue tests have been performed with Aluminium alloy specimens contacting with steel pads. Friction force response and fatigue crack growth were monitored under a wide range of axial load and static normal load. An attempt is made to present the crack growth results using linear elastic fracture mechanics parameters, by correlating with the elastic stress intensity factors for mode I and mode II. The results indicate that in some tests fretting cracks of the order of grain size can be detected at as early as 10-20 percent of the fatigue life, and the fracture process is seen to be dominated by progressive crack growth. A characteristic crack path is observed in fretting, where cracks initially grow on a plane inclined to the applied axial load, assumed to be in mixed-mode (mode I and mode II), attaining a considerable size before they turn to a mode I plane. The crack growth results for various combinations of axial load and static normal load are correlated using K_I and K_{II}, taking into account the experimentally observed crack path.

KEYWORDS

Fretting, fatigue, friction force, crack growth, contact pressure, fracture mechanics, mixed mode.

INTRODUCTION

Fatigue failure originated by fretting is commonly observed in assemblies where surfaces of two components are in contact and small relative movement can exist between them. In a fretting situation, the stress singularity caused by the contact pressure and the friction force at the edge of the contact patch will speed up the crack nucleation process and accelerate the early phase of crack growth. This often results in significant reduction of fatigue endurance and fatigue strength. It has been shown by a number of investigations [Endo, 1981; Sato et al, 1986, Fernando et al, 1993a] that significant fretting cracks may be detected at very early stage, in some instances as early as 10-20 percent of fatigue life, indicating that the fretting fatigue fracture is dominated by progressive stable crack growth. Therefore fracture mechanics methodology is considered to provide an ideal tool for characterisation of the fretting fracture processes. In situations where only microscopic yielding occurs in the vicinity of the contact zone, as is the case for many situations of fretting fatigue, linear elastic fracture mechanics (LEFM) is believed to be adequate and the elastic stress intensity factor (SIF) may be an appropriate parameter for the characterisation of fretting crack growth behaviour.

LEFM has been used in the past by many researchers, with reasonable success, to predict fretting fatigue life [Edwards, 1981, Sakata et al, 1986, Faanes and Fernando, 1993]. In almost all of these analyses an arbitrary crack path was assumed and only pure mode I crack growth was considered. Only a few investigations so far have been involved with measuring growth of fretting fatigue cracks, and limited attempt is made to predict crack growth behaviour in terms of LEFM [Troshchenko et al, 1988]. As shown by many experimental results [Rayaprolu and Cook, 1992], a characteristic crack path is observed in fretting, where cracks initially grow on a plane inclined to the applied axial load to a considerable size before they turn to follow an obvious mode I plane, which is normal to the applied axial load. This initial phase of growth is assumed to be in mixed-mode, i.e. combined mode I and mode II. Since a major part of fretting fatigue life is spent propagating the inclined crack, any proper analysis for prediction of fretting crack growth or fretting fatigue life should take into account the influences of the crack path and mixed-mode behaviour of crack growth. In this paper an attempt is made to correlate experimentally observed crack growth results, for various combinations of fretting loading, using values of K_I and K_{II} that take into account the observed crack path, where K is the associated SIF.

EXPERIMENTAL PROCEDURE

The loading arrangement used for the present investigation is schematically illustrated in Fig. 1. The loading facility used was primarily developed for the purpose of performing variable normal load fretting tests and is described in detail elsewhere [Fernando et al, 1993b]. The specimen is fixed between two horizontally placed servo-controlled actuators, so that the specimen can be subjected to cyclic axial load. The pads are symmetrically clamped to the specimen on both sides as shown, and normal load is applied via a set of vertically placed servo-controlled actuators. The pad bridge consists of two feet, providing flat contacts to create fretting action. Each pad bridge is kept in position on the specimen by using two symmetrically placed locating arms which are connected to the specimen grips. In this arrangement the slip amplitude (amplitude of the relative movement at the contact) is determined by changing the amplitude of axial load and the pad span; i.e. the distance between the two feet of the bridge. The signals from strain gauges bonded to the pad bridges were used to measure the friction forces. The axial load of the specimen and the normal load on the contact area were measured from the loadcells attached to the respective actuators.

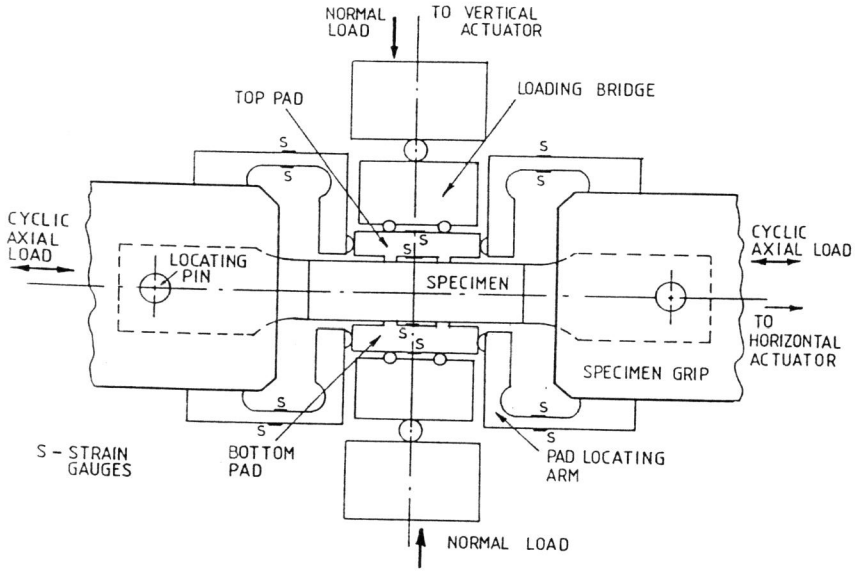

Fig. 1. Fretting fatigue loading arrangement.

The material investigated was a fully artificially aged 4% Copper Aluminium Alloy, a general purpose material widely used in aerospace/aircraft structures and components. The fretting pads were made of BS S98 steel. All tests were performed with axial load at mean zero and with a sinusoidal waveform of 15 Hz frequency. During the test programme three pad spans were tested (6.35 mm, 16.5 mm and 34.35 mm), together with three axial stress amplitudes; 70 MPa, 100 MPa and 125 MPa. Tests were performed with various values of normal pressure, covering the range 20 MPa to 120 MPa. However in this paper only the results of the 16.5 mm pad span are considered.

During the experiments, the fretting crack growth in the specimens was measured using a direct current potential drop method. The details of the crack measuring technique are given elsewhere [Fernando et al, 1993a]. A personal computer based data acquisition system was used to record axial load and friction force hysteresis loops and potential drop measurements during tests.

EVALUATION OF MODE I/II STRESS INTENSITY FACTORS

The elastic stress intensity factors for fretting cracks have been developed from the Finite Element (FE) method. A FE model based on the experimental loading arrangement, the representative of the specimen-pad loading interaction as shown in Fig. 2a, was developed and used to obtain the values of both K_I and K_{II} for various combinations of crack length, ($0 < a \leq 2$ mm) and crack angle, ($0 < \theta < 45$ deg.). The evaluations were performed for three unit load cases; unit axial load, unit normal load and unit friction force, and for a number of contact load distributions [Sheikh et al, 1993]. For the present analysis a uniform normal load and friction force distribution under the pad contact was assumed. The numerical values obtained by the FE method have been used to evaluate K_I and K_{II} for the loads corresponding to each test, as follows.

The numerically obtained K_I and K_{II} values of individual unit load cases were curve fitted by polynomial functions with two variables a and θ. These equations in turn were used together with experimentally recorded data for axial load, normal load and friction force to evaluate SIFs at each recorded data point of the loading cycle. The variation of the values of K_I and K_{II} during the loading cycle have been used to evaluate the range, mean and maximum values of the SIFs, for different values of crack lengths and crack orientations. For each test, data for a loading cycle which corresponded to the stable friction response was selected for analysis.

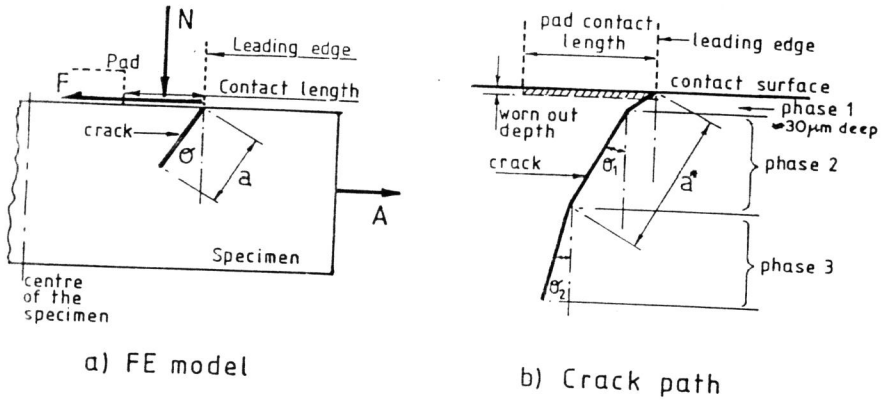

Fig. 2. Fretting cracks, a) FE model, b) crack path

CRACK GROWTH RESULTS AND CRACK PATH DETAILS

The potential drop measurements recorded during the progress of tests clearly indicated that the growth of fretting cracks could be detected by this method at a very early stage of fatigue life when compared with that of ordinary fatigue at similar stress values. It was also observed that the higher the value of friction force, the earlier the cracks could be detected [Fernando et al, 1993a], and at 120 MPa normal pressure, where the highest friction force is achieved, the cracks were detected as early as 10-20 percent of the fatigue life. This clearly indicates the critical damage influence of the friction force at early stages of fretting crack growth. The evolution of the friction force during tests has indicated that a rapid increase in friction amplitude occurs during this early stage. The highest friction amplitude was achieved at approximately 5-10 percent of the lifetime, and during subsequent loading the friction amplitude was found to be more or less constant.

For the case of a 16.5 mm pad span typical crack growth results are shown in terms of crack growth rate versus crack length, a, in Fig. 3. The results are presented for three different values of normal pad pressure,

20 MPa, 80 MPa and 120 MPa, and for the three values axial load amplitude used. The friction amplitudes observed in these tests are given in Table. 1. The LEFM prediction of the crack growth curve for the material [Pearson, 1973], corresponding only to the respective values of axial load, is also shown in the figure. The LEFM lines correspond to the stress ratio R= 0, where R is the ratio of minimum to maximum stress of the loading cycle.

Observation of the fracture area of the specimen reveals that in all tests the cracks, in particular the main crack that caused final failure, originated at or very near to the leading edge of the contact patch. In many tests multiple cracks were observed to grow from different contact locations. This was expected as the all four contact locations were equally loaded. In a few tests though, cracks were originated at the side faces of the leading edge and grew as corner cracks. In the majority of tests multiple cracks nucleated along the leading edge. These cracks eventually grew with a semi-elliptical crack front. Observation of the contact patch indicated that less severe contact was achieved near to the side faces of the specimen, and the crack path on the side faces of the specimen was found to be different to that observed at an inner section. This is thought to be due to influence of stress/strain state, where plane stress conditions exist at the side faces compared to plane strain expected at the middle section. Therefore crack path details were measured on a plane 2 mm away from the side faces. This was thought to provide a representative crack path.

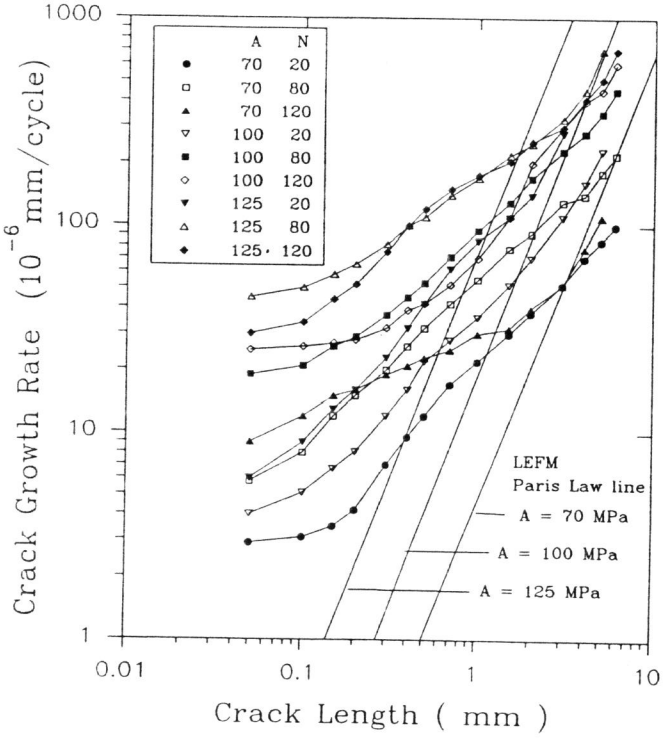

Fig. 3. Fretting fatigue crack growth results for BS L65 Aluminium alloy

The fractured specimens showed consistent crack path behaviour, which is schematically illustrated in Fig. 2b. In almost all tests the crack was found to nucleate at a steep angle approximately 45 to 60 degrees to the normal axis, and this initial growth continued to a depth of up to about 30μm. In many tests the major part of

the crack for this initial phase (phase 1) was not visible as it was within the worn-out depth of the scar. The crack then turned to a plane with a less steep angle between 10 to 30 degrees to the normal axis. The subsequent crack growth (phase 2) was found to be quite straight and up to a significant length, a^*, of the order of 0.4 to 0.9 mm. Finally the crack turned to a plane normal or very close to the normal to the applied axial load (phase 3). In many tests the transition from phase 2 to 3 was found to be gradual and over a 0.2-0.3 mm distance. The crack path information for each test is given in the Table 1.

Table 1. Details of loading and crack path

Test No.	A (MPa)	N (MPa)	F (MPa)	a* (mm)	θ_1 (deg.)	θ_2 (deg.)
126	70	20	36	0.52	21	0
123	100	20	39	0.46	25	2
129	125	20	34	0.40	28	0
127	70	80	74	0.93	18	4
124	100	80	84	0.46	22	3
128	125	80	98	0.75	19	0
134	70	120	77	0.21	27	4
125	100	120	79	0.34	25	3
130	125	120	118	0.43	22	5

DISCUSSION

From Fig. 3 it can be seen that for all cases of tests, a significant increase in growth rate is evident at crack lengths below 2 mm in fretting when compared with the growth rate predicted by LEFM using only the axial load. Comparing the magnitudes of friction forces encountered in these tests, it can be clearly seen that this increase in the growth rate is primarily due to the influence of friction force. The influence of the normal load on crack growth rate is also evident, causing the considerable retardation in growth rate observed under 120 MPa normal pressure. The retardation effect due to normal pressure was more pronounced at medium crack lengths, indicating that this may probably be due to crack closure under high compressive normal load.

In Fig. 4 the crack growth results are correlated using the range of mode I stress intensity factor, ΔK_I. The same results are presented in terms of maximum K_I in Fig. 5. For both these figures the actual crack path was used in the evaluation of K_I. By comparison with Fig. 3, it can be seen that a major part of the enhancement of growth rate, in particular at medium crack length, is accounted by the use of friction force and the normal load in the evaluation of K_I. However increased growth rate and deviation from mode I material behaviour; i.e. Paris law line, is still visible at smaller crack lengths. The presence of the experimental data below the material data line in Fig. 4 can be explained by the influence of the negative stress ratio encountered in fretting. The typical values of the stress ratio observed in the present tests fall within -1.4 to -2.8. The higher value quoted is encountered at small crack lengths and the value gradually reduces as the crack length is increased. The better correlation of the test results with the material data seen in Fig. 5, at higher crack lengths (a > 1 mm), is expected as the use of maximum K will take into account the effect due to crack closure, if the mode I crack opening stress is assumed to be zero.

Crack growth results, up to 2 mm crack length are presented in terms of the ΔK_{II} in Fig. 6. The mode I material behaviour is given in the figure for comparison purposes only. In Fig. 6a and 6b the results are correlated in terms of the ΔK_{II}, for crack angles 0 and 45 degrees, respectively. In Fig 6c the results are presented in terms of the maximum value of the ΔK_{II} out of the above two crack angles. As seen from these figures, the values of ΔK_{II} are significantly altered by the crack angle used in the analysis. At very short crack lengths a better correlation is achieved for a 45 degree crack angle. The best overall correlation is shown by Fig. 6c for the whole range of crack lengths. The results in terms of the ΔK_{II} for the actual crack path are presented in Fig. 6d. The fact that some lower ΔK_{II} values are observed for actual crack path, compared to 0 and 45 degrees crack angle, indicates that although the cracks grow in mixed-mode, the plane of the phase 2 crack growth is not far removed from the mode I plane in some instances. This may be a reason for the wide scatter observed in Fig.6d. As seen from the Fig. 6d, for some tests in particular at higher

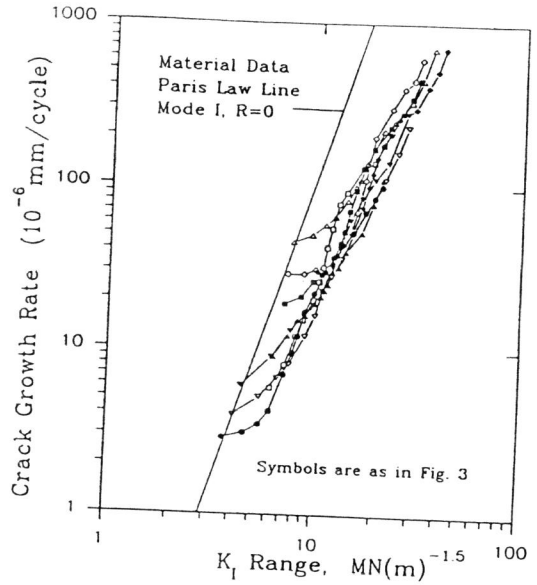

Fig. 4. Predicted and experimental crack growth results for mode I cracking.

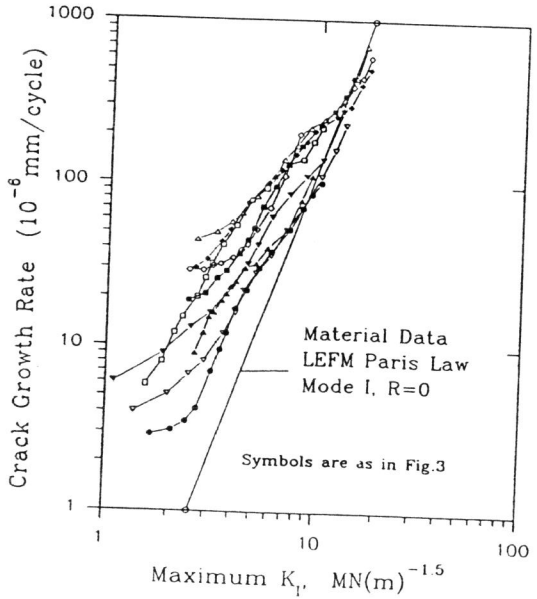

Fig. 5. Crack growth prediction allowing for mode I closure of long cracks.

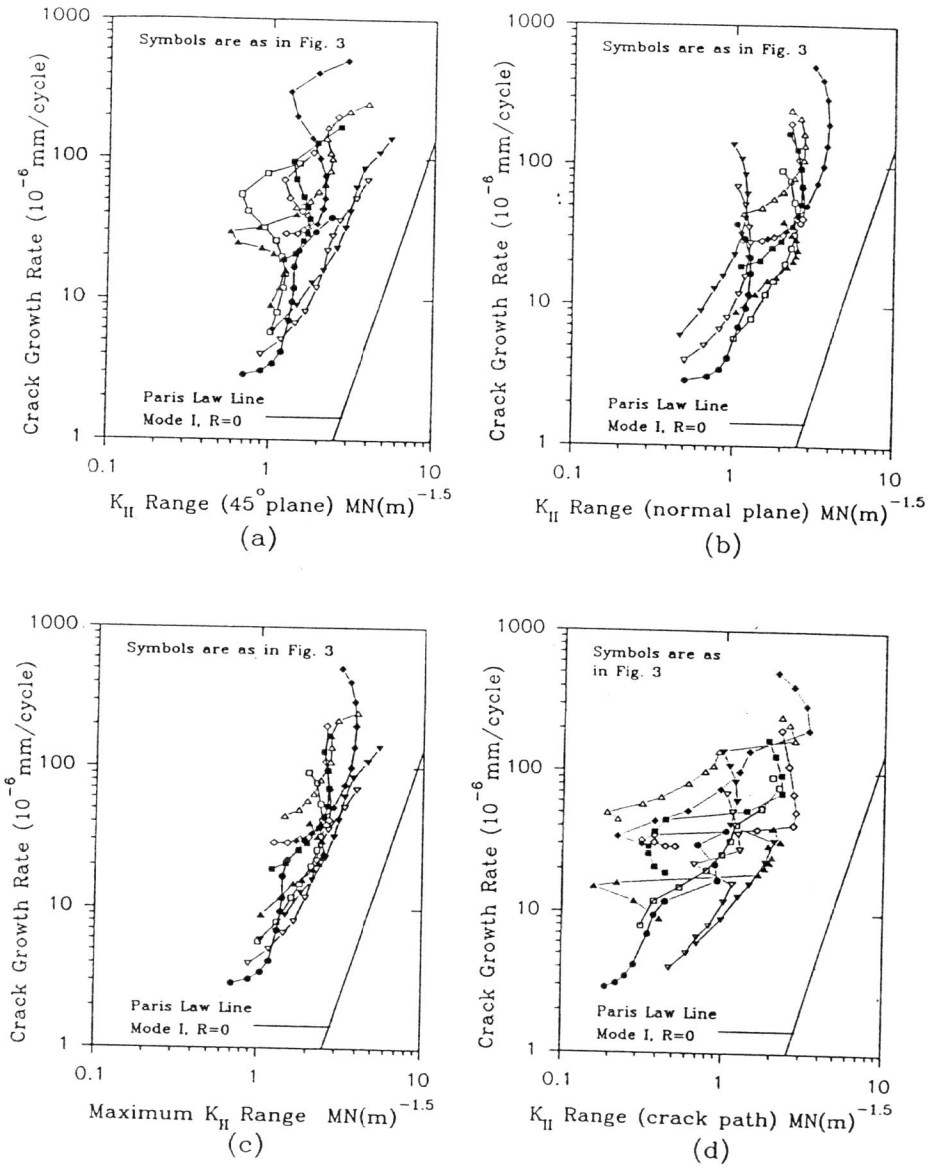

Fig. 6. Mode II contribution to crack growth, a) for 45° crack path, b) for normal crack path, c) maximiized mode II SIF range, and d) for observed crack path (phase 2)

axial load amplitudes, the growth curve shows a negative gradient at the beginning of the curve. This suggests that for these tests mode I growth becomes dominant from fairly short crack lengths. The mode II influence seen to dominate at lower axial stress amplitudes. The possible mode II dominated growth regions are shown with solid lines in the figure. However more detailed analysis is needed before drawing a firm conclusion.

In general the lack of proximity of the experimental results at short crack lengths to the mode I line in Fig. 5 indicates the degree of mixed-mode interaction in crack growth. Since phase 3 cracks are entirely mode I above 2 mm in length, the mode II contributions in Fig. 6d must fall to zero for higher crack lengths and propagation rates.

CONCLUSION

Fretting fatigue crack growth rate for a wide range of axial and normal load have been correlated using mode I and II SIFs, taking into account the observed crack path. The crack growth results for higher crack lengths (a > 1 mm) are better correlated by K_I maximum, allowing for the closure effect. The values of ΔK_{II} are significantly altered by the crack angle used in the analysis. The inclined crack path observed in fretting seem to be closer to the mode I path, in particular at higher axial stress amplitudes. The mixed-mode influence seen to dominate at lower axial stress amplitudes, though more detailed analysis is needed before making a firm conclusion.

Acknowledgements - The authors gratefully acknowledge RAE, Farnborough and the SERC (UK) for funding this investigation. Special thanks are due to Mr. R. Cook, Dr. D. Rayaprolu, Dr. R. B. Waterhouse for their advice. The authors are indebted to Dr. G. H. Farrahi and Mr. B. Platt for their valuable role in the experimental programme, and to the University of Sheffield for providing financial support (USF).

REFERENCES

1. P. R. Edwards (1981), The application of fracture mechanics to predicting fretting fatigue, "Fretting Fatigue", Ed. R. B. Waterhouse, pp. 67-98
2. K. Endo (1981), Practical observation of initiation and propagation of fretting fatigue cracks, "Fretting Fatigue", Ed. R. B. Waterhouse, pp. 127-142
3. S. Faanes and U. S. Fernando (1993) Life prediction in fretting fatigue using fracture mechanics, Proc. Int Conf of Fretting Fatigue, Sheffield, UK.
4. U. S. Fernando, G. H. Farrahi and M. W. Brown (1993), Fretting fatigue crack growth behaviour of BS L65 Aluminium Alloy under constant normal load, Proc. Int Conf of Fretting Fatigue, Sheffield, UK
5. U. S. Fernando, M. W. Brown, K. J. Miller, R. Cook and D. Rayaprolu (1993), Fretting fatigue behaviour of BS L65 Copper Aluminium Alloy under variable normal load, Proc. Int Conf of Fretting fatigue, Sheffield, UK.
6. S. Pearson (1973) Initiation of fatigue cracks in commercial Aluminium Alloy and the subsequent propagation of very short cracks, RAE Report No. 72236, RAE, Farnborough, UK.
7. D. Rayaprolu and R. Cook (1992), A critical review of fretting fatigue investigations at the Royal Aerospace Establishment, Standardization of Fretting Fatigue - Test methods and equipment, M. H. Attia and R. B. Waterhouse, Eds., ASTM STP 1159, ASTM, Philadelphia.
8. H. Sakata, T. Hattori and T. Hatsuda (1986), An application of fracture mechanics to fretting fatigue analysis, Proc. Int. Conf. on Role of fracture mechanics in modern technology, Kyushu, Japan
9. K. Sato, H. Fujii and S. Kodama (1986), Crack propagation behaviour in fretting fatigue of S45C steel, Bulletin of JSME, Vol. 29, No. 256, pp. 69-77.
10. M. A. Sheikh, U. S. Fernando, M. W. Brown and K. J. Miller (1993), Elastic stress intensity factors for fretting cracks using the Finite Element method, Proc. Int Conf of Fretting Fatigue, Sheffield, UK.
11. V. T. Troshchenko, G. V. Tsybanev and A. O. Khotsyanovskii (1988) Life of steels in fretting fatigue, Problemy Prochnosti, (in Russian), No. 6, June 1988, pp. 3-8.